Novel *in-situ* lamella fabrication technique for *in-situ* TEM

Megan Canavan [a,b,c], Dermot Daly [b,c], Andreas Rummel [d], Eoin K. McCarthy [b,c], Cathal McAuley [b,c], Valeria Nicolosi [b,c,e,*]

[a] *School of Physics, Trinity College, Dublin, Ireland* [b] *CRANN, TCD – Trinity College, Dublin, Ireland* [c] *AMBER, TCD – Trinity College, Dublin, Ireland* [d] *Kleindiek Nanotechnik GmbH, Reutlingen, Germany* [e] *School of Chemistry, Trinity College, Dublin, Ireland*

a r t i c l e i n f o

Article history:
Received 3 August 2017
Revised 22 March 2018
Accepted 28 March 2018 Available online 29 March 2018

Keywords:
Focused ion beam
Lamella preparation
In-situ heating
Lift-out
Low-kV milling

a b s t r a c t

In-situ transmission electron microscopy is rapidly emerging as the premier technique for characterising materials in a dynamic state on the atomic scale. The most important aspect of *in-situ* studies is spec- imen preparation. Specimens must be electron transparent and representative of the material in its op- erational state, amongst others. Here, a novel fabrication technique for the facile preparation of lamellae for *in-situ* transmission electron microscopy experimentation using focused ion beam milling is devel- oped. This method involves the use of rotating microgrippers during the lift-out procedure, as opposed to the traditional micromanipulator needle and platinum weld. Using rotating grippers, and a unique ad- hesive substance, lamellae are mounted onto a MEMS device for *in-situ* TEM annealing experiments. We demonstrate how this technique can be used to avoid platinum deposition as well as minimising dam- age to the MEMS device during the thinning process. Our technique is both a cost effective and readily implementable alternative to the current generation of preparation methods for *in-situ* liquid, electrical, mechanical and thermal experimentation within the TEM as well as traditional cross-sectional lamella preparation.

© 2018 Elsevier B.V. All rights reserved.

1. Introduction

As the dimensional requirements of device materials shrink, the need to understand and manipulate materials at the single-atom level has become critical for an ever-increasing range of technolo- gies. Transmission electron microscopy (TEM) has emerged as the primary tool for exploring materials on the nanoscale. Real-time observations of materials undergoing dynamic changes upon the application of external stimuli are increasingly recognised as vi- tal to understanding the fundamental processes taking place dur- ing materials synthesis, processing and functioning [1] . In techno- logical applications, a material is exposed to a variety of environ- mental stress and external stimuli. The response of a material to these stimuli often influences their functionality. Based on this rea- soning, *in-situ* TEM has become an essential technique within the field of material science. *In-situ* techniques such as annealing [2] , biasing [3] , cryogenics [4] , liquid/gas [5–7] , mechanical interroga- tion [8,9] and electrochemical analysis [10] , have been developed to track the evolution of materials under such external stimuli.

Thermal experimentation within the TEM has provided a new and interesting perspective on many material sets [11–14] . *In-situ* annealing has progressed from heating entire sample grids to using Micro-Electro-Mechanical Systems (MEMS) devices to enable lo- calised heating. This technology provides greater temperature con- trol due to the small volume and reduced thermal mass of the heater. Moreover, it considerably reduces specimen drift and set- tling time [15] . The use of this technology for *in-situ* annealing ex- periments has enabled the process to become fast and reliable, of- fering new insights into material morphology [16,17] . Despite all the progress that has been made using *in-* situ annealing experi- ments, studying dynamic processes *in-situ* within the TEM presents several important challenges, including specimen preparation and sample transfer.

The methods described in this paper outline an innovative and reproducible technique to cross-section lamella preparation for *in- situ* experimentation using a gallium (Ga) + Focused Ion Beam (FIB), as well as an improved method for mounting electron-transparent lamellae directly onto a research platform – in this case, the MEMS device. This is an improved technique over that of preparing larger, bulk-like sample sizes, which generally leads to anisotropic heat distribution throughout the sample.

* Corresponding author at: CRANN, TCD – Trinity College, Dublin, Ireland. *E-mail address:* nicolov@tcd.ie (V. Nicolosi).

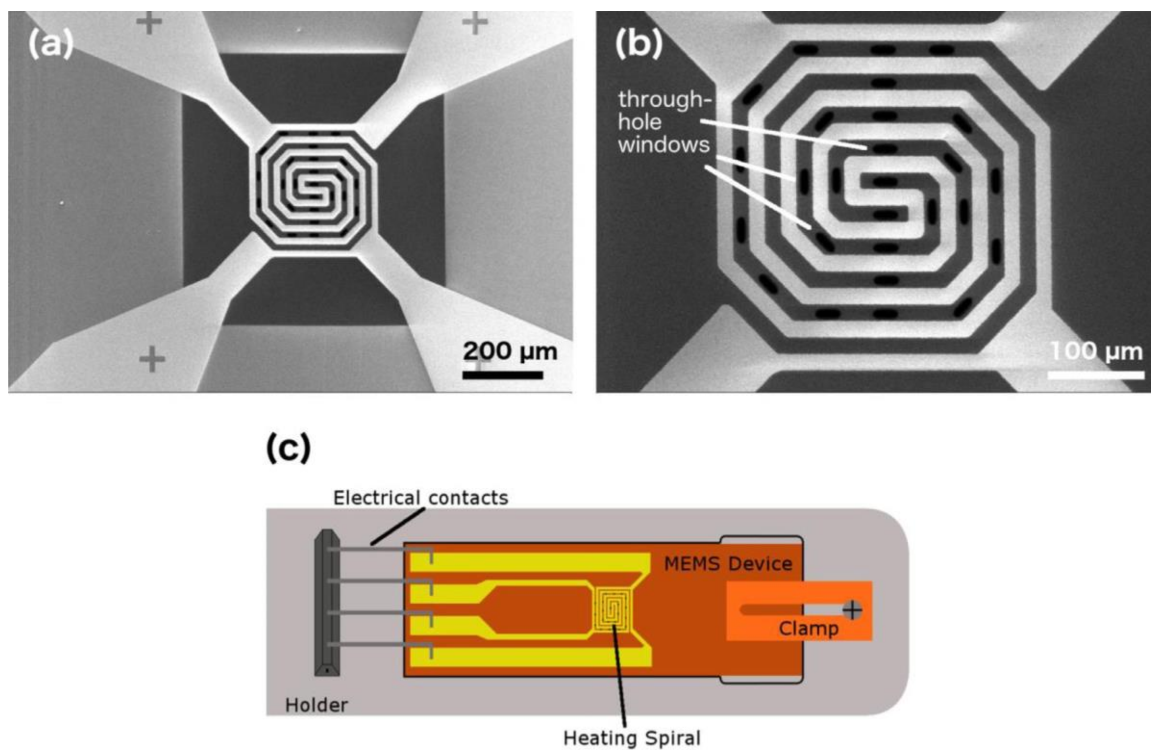

Fig. 1. (a) SEM image of MEMS device displaying the 4-point geometry, (b) SEM image of MEMS device showing the heating spiral and through-hole windows and (c) schematic of heating holder and MEMS device.

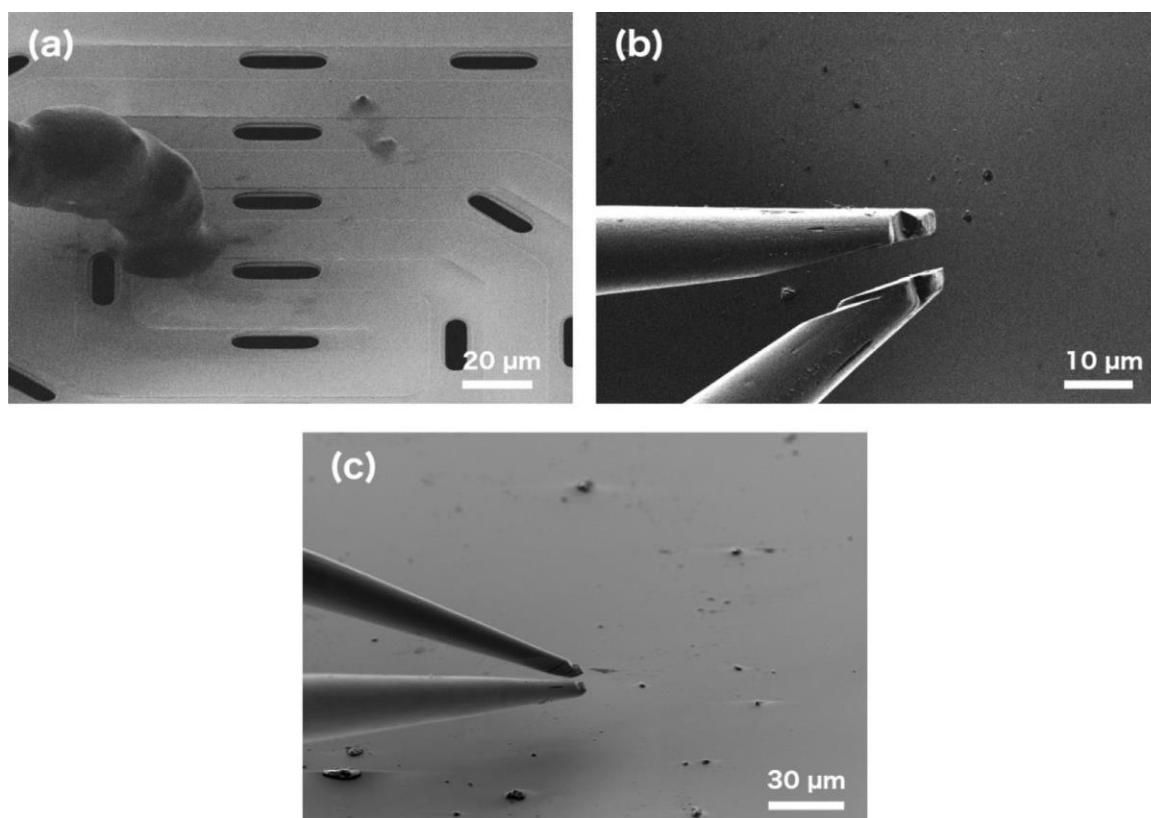

Fig. 2. (a) SEM image showing the application of SEMGlu around the surrounding windows of the MEMS device using a micromanipulator needle, (b) and (c) FIB and SEM images respectively showing the correct positioning of the microgrippers prior to lift-out.

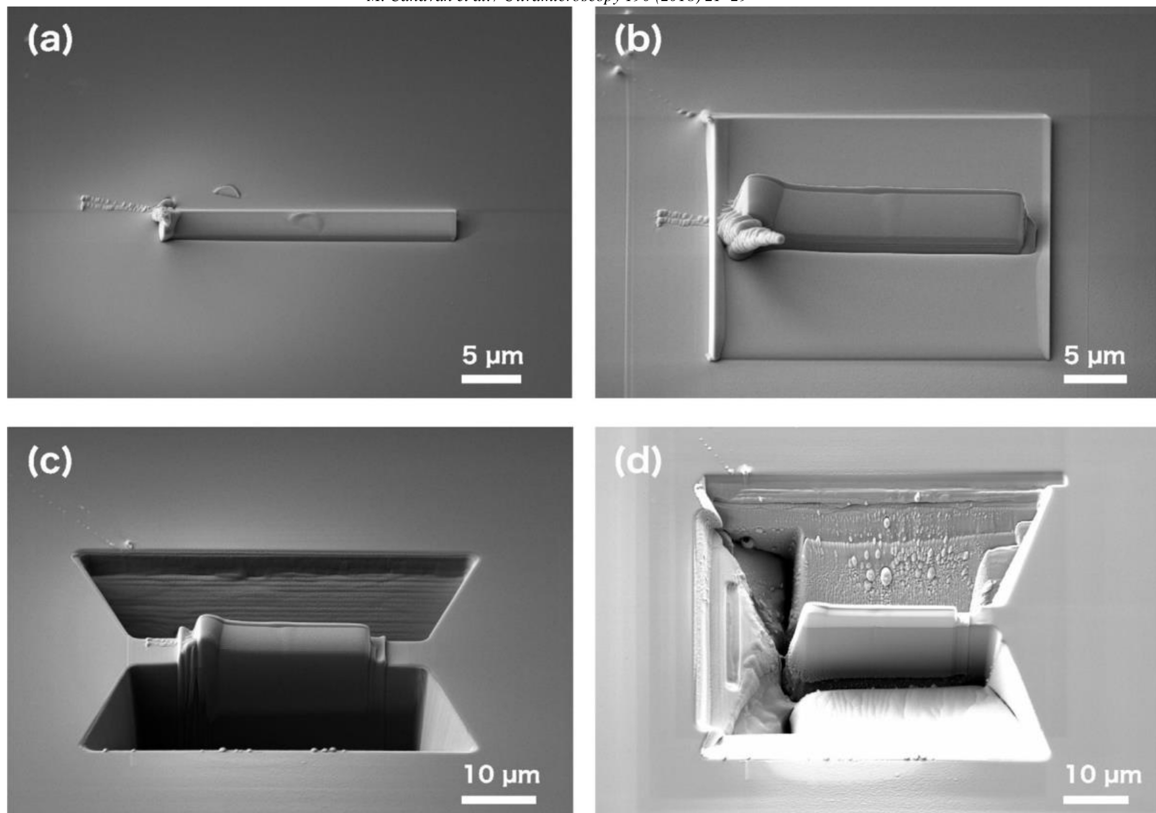

Fig. 3. SEM images showing overview of bulk preparation for lamella lift-out: Protective Pt strip deposited by (a) electron beam-induced deposition and (b) ion beam-induced deposition, (c) two trapezoid trenches milled to a depth of approximately 15 µm, and (d) side trench and undercut viewed at 20 ° stage tilt.

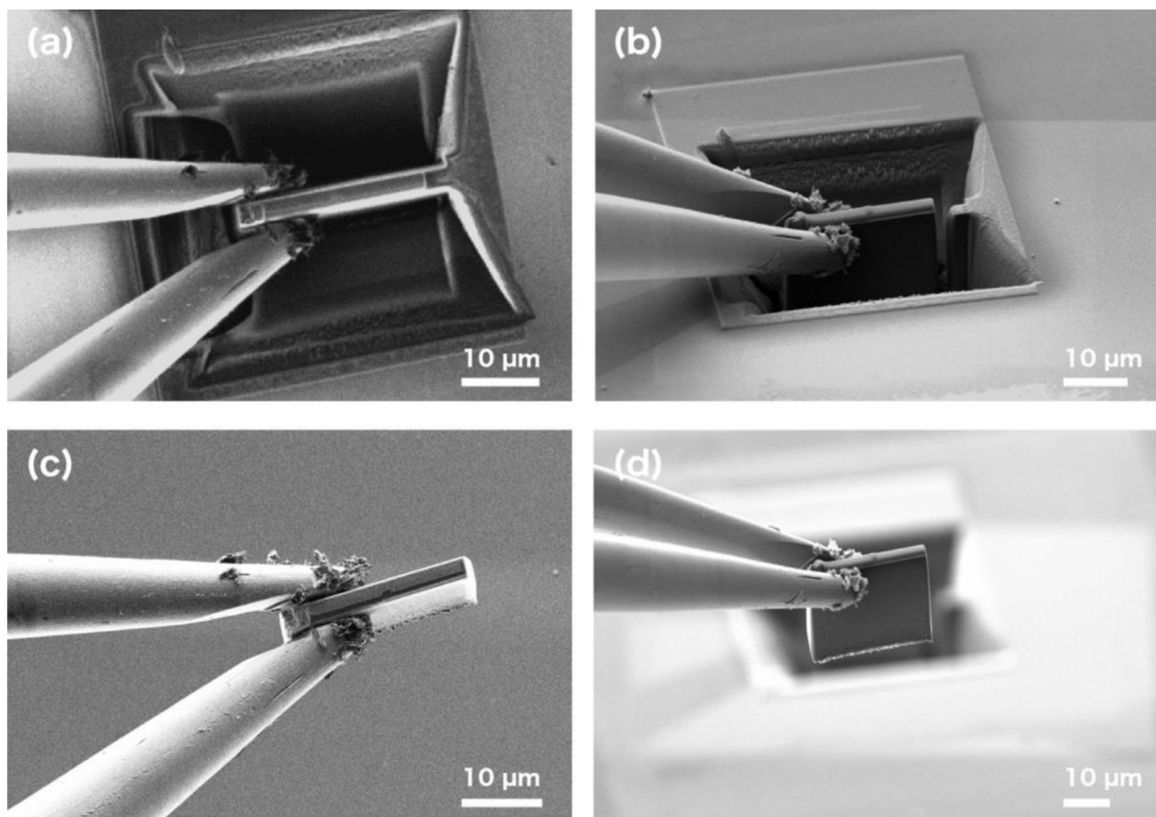

Fig. 4. (a) FIB image of lamella securely gripped, (b) SEM image of milling sidewall connecting to bulk sample, (c) and (d) FIB and SEM images respectively of the positioning of lamella during the thinning process.

Table 1
Complete set of parameters for lamella preparation.

Preparation Step	Primary Mode	SEM Voltage	E-Beam Current	FIB Voltage	I-Beam Current	Depth	Tilt	Details
MEMS device preparation	Imaging: e-beam	5 kV	3 nA				54 °	Using the manipulator needle, SEMGlu is applied carefully around the windows of the MEMS device
EBID-Pt	Deposition: e-beam	5 kV	3 nA			0.5–1 µm	54 °	Thickness of 2 µm × 22 µm
IBID-Pt	Deposition: i-beam	5 kV	3 nA	30 kV	20 pA	1.5–2 µm	54 °	Thickness of 2 µm × 22 µm
Trenches	Milling: i-beam	5 kV	3 nA	30 kV	4 nA	15 µm	54 °	Dimensions of 40 µm × 50 µm × 15 µm
Side Trench	Milling: i-beam	5 kV	3 nA	30 kV	4 nA	15 µm	54 °	Dimensions of 30 µm × 10 µm
Undercut	Milling: i-beam	5 kV	3 nA	30 kV	2 nA	3–4 µm	7 °	Dimensions of 1 µm × 24 µm
Final sidewall removal	Milling: i-beam	5 kV	3 nA	30 kV	2 nA	15 µm	54 °	Dimensions of 2 µm × 2 µm
Lamella lift-out	Imaging: e-beam	5 kV	3 nA	30 kV	20 pA		54 °	Sample lifted out using microgrippers
Thinning in RoTip microgrippers – Stage 1	Milling: i-beam	5 kV	3 nA	30 kV	240 pA		58 - 59 °	Milled to a thickness of approximately 70 0–80 0 nm (4 – 5 ° tilt with respect to FIB)
Thinning in RoTip microgrippers – Stage 2	Milling: i-beam	5 kV	3 nA	15 kV	200 pA		58 - 59 °	Milled to a thickness of approximately 20 0–30 0 nm (4 – 5 ° tilt with respect to FIB)
Thinning in RoTip microgrippers – Stage 3	Milling: i-beam	3/5 kV	3 nA	5 kV	20 pA		57 - 58 °	Milled to a thickness of approximately 50–70 nm (3 – 4 ° tilt with respect to FIB)
Transfer of lamella to device	Imaging: e-beam/i-beam	3 kV	10 pA	30 kV	20 pA		0 °	Lamella and MEMS device both at coincidence point. SEM voltage and beam current lowered to reduce charging and prevent any unnecessary curing of the SEMGlu prior to the final stages of the transfer.
Securing lamella over MEMS device window	Curing: e-beam	30 kV	6 nA				0 °	Lamella successfully placed over the window. Thicker end of lamella over SEMGlu exposed to a high beam voltage for approximately 30 minutes to ensure a secure placement.

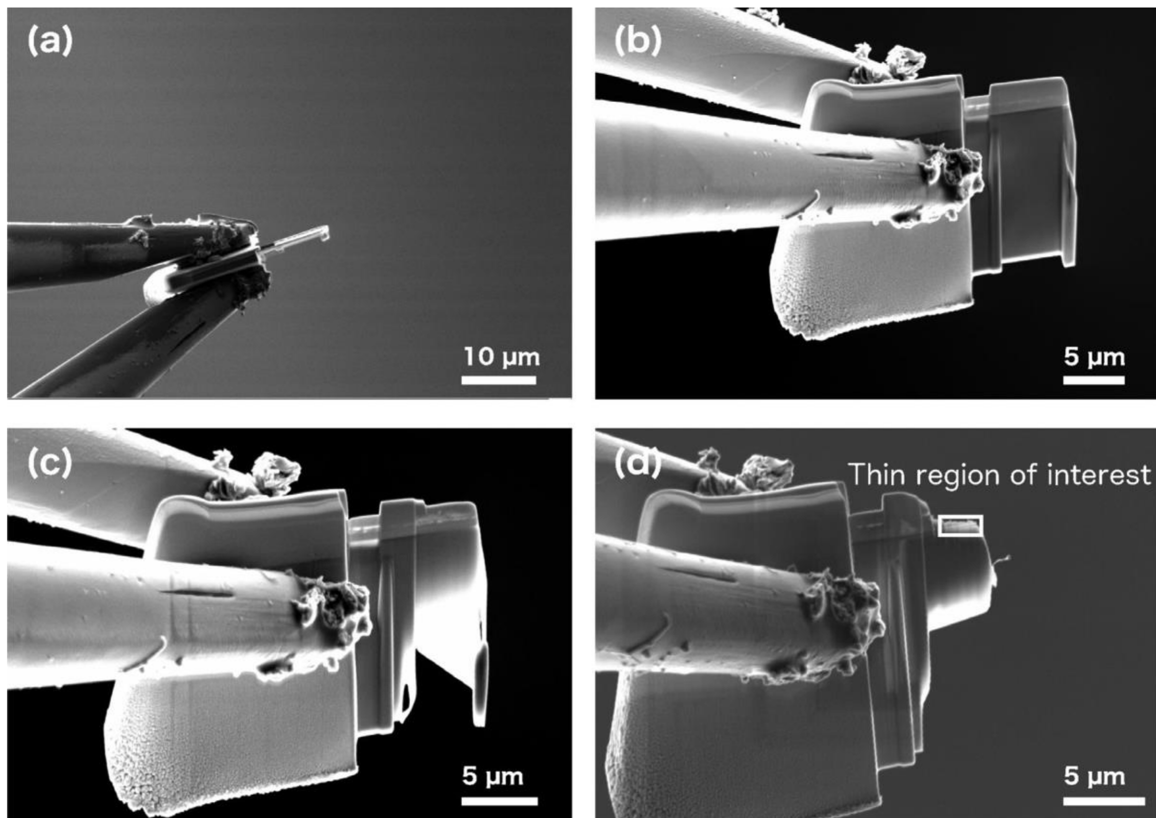

Fig. 5. (a) and (b) FIB and SEM images respectively showing the staggered approach to the thinning process, allowing the thicker segment to create a ledge between the thinned section of the lamella and the surface of the MEMS device, (c) and (d) SEM images of the final thinning stages 15 kV 200 pA and 5 kV 20 pA respectively with thin region of interest highlighted.

FIB sample preparation is a well understood and frequently used technique, as it is an efficient and reliable method for prepar- ing high-quality electron-transparent samples with minimal dam- age [18–23] . A method for lamella lift-out for MEMS device mount- ing has been developed previously [24] . In the technique presented here lamella transfer is achieved by the chemomechanical secur- ing of the lamella to the MEMS device, eliminating the need to use the platinum (Pt) weld technique. Avoiding the use of elec- tron beam-induced deposition (EBID)-Pt comes with two distinct advantages: 1) no re-deposited platinum spray from the deposi- tion process, which would contaminate the lamella; and 2) no risk of damaging the MEMS device during the thinning process.

The technique detailed in this paper not only provides a new improved lamella preparation method for *in-situ* annealing, but also presents a novel means for preparing cross-sectional lamellae for applications across many different analytical platforms.

2. Experimental methods

The technique utilises a Zeiss Auriga cross-beam FIB-SEM sys- tem for complete lamella fabrication as well as lamella transfer to the MEMS device. (MEMS devices were purchased from DENSsolu- tions). All FIB and SEM images shown within the main text were recorded on a Zeiss Auriga FIB-SEM. The SI video was recorded on an FEI Quanta 200 3D. The MEMS device consists of a molybde- num (Mo) spiral encapsulated between two SiN_x membranes. The Mo spiral heats the localised area via joule heating controlled by a 4-point probe feedback loop. As well as the Mo heating spiral, there are a series of through-hole windows (5–20 µm) [25] . The lamella is positioned over a window close to the centre of the heating spiral as shown in Fig. 1 . The MEMS device can reach a maximum temperature of 1300 °C, with temperature stability of < 1 °C at 1300 °C. It has a heat rate of 200 °C per millisecond and a settling time of < 2 seconds.

Our standard proof-of-concept specimen is bulk silicon (Si) for reproducible, reliable fabrication and analysis. SEMGlu (Kleindiek Nanotechnik GmbH, Reutlingen) was used for securing lamellae to the MEMS device. SEMGlu is a vacuum-compatible adhesive that is cured by electron-beam irradiation, providing a mechanically ro- bust and thermally stable bond between the lamella and the MEMS device [26] .

A reduced electron-beam current of ~10 pA permits working with the glue under Scanning Electron Microscope (SEM) obser- vation. Adhesive curing is achieved by irradiating with the con- densed electron probe for one minute, using a beam current den- sity of 10 pA/µm ^{2} on the SEMGlu, causing the adhesive to harden. The incident electrons trigger a polymerisation process and change the physical properties of the glue (elasticity, tensile strength). The electron-beam voltage determines the penetration depth (approx- imately 100 nm per kV) into the glue and thus the glue's curing volume.

The application of the SEMGlu and the removal of the lamella are performed using a roof-mounted Kleindiek micromanipulator fitted with RoTip and microgrippers for lamella lift-out. The ROTIP- EM is a rotational axis plug-in for the MM3A-EM micromanipulator that enhances the system by providing a fourth degree of freedom, which is ideal for this particular technique.

In this study we use a DENSsolutions Wildfire S3 heating holder, however the technique is compatible with other heating holders. The system comprises of a single tilt holder with the MEMS device replacing the standard TEM grid. The TEM holder has a tilt range of + / −30 ° with maximum sample drift of 0.5 nm/min

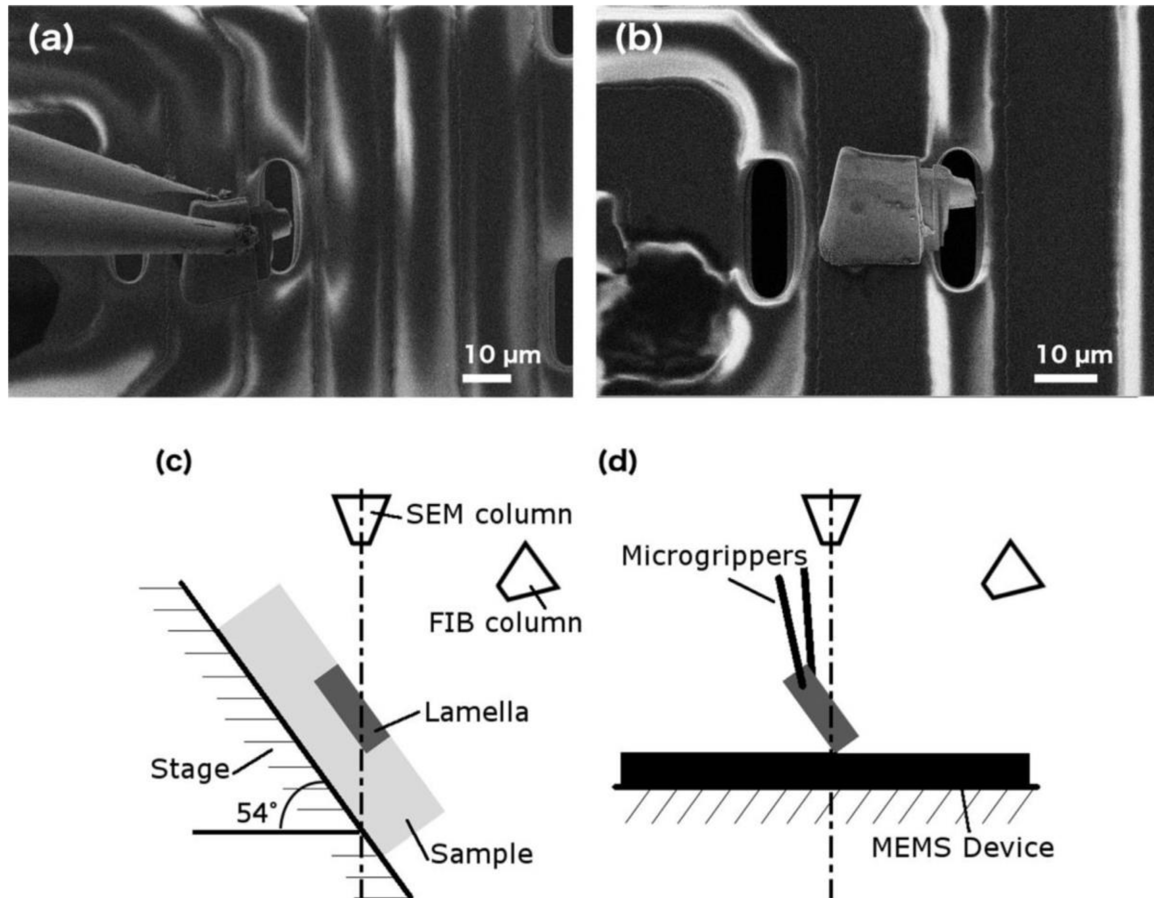

Fig. 6. SE M images of (a) the transfer of the lamella from the grippers to the MEMS device, (b) the high-kV curing of the lamella and SEMGlu, (c) and (d) schematics of lift-out geometry.

at 800 °C. S/TEM imaging and analysis is performed on a FEI Titan TEM at 300 kV.

3. Protocol for novel fabrication technique

The fabrication process begins by mounting a through-hole MEMS device on to a standard SEM stub using carbon adhesive. A separate reservoir of SEMGlu is also placed in the chamber away from the MEMS device. Before the lamella is placed on the area of interest, the MEMS device is pre-loaded with SEMGlu. A micro- manipulator needle is dipped into the SEMGlu reservoir forming a teardrop-shaped portion at the tip of the needle. The needle is driven to the MEMS device and lowered until the SEMGlu makes contact with the SiN_x surface. The stage is slowly moved in the x and y direction to gently disperse the SEMGlu around the desired windows, Fig. 2 (a). As can be seen from Fig. 2 (a), dispersing the glue around several windows provides a greater number of loca- tions for mounting the lamella, increasing the success rate of the lift-out.

After SEMGlu application the needle is replaced with the mi- crogrippers and RoTip attachment, providing full 360 ° rotation. Fig. 2 (b) and (c) show FIB and SEM images of the correct posi- tioning of the grippers with respect to the lamella. For accurate positioning of the microgrippers during lift-out, they are tilted to 54 °, parallel to the FIB, using the RoTip.

The bulk lamella preparation was based on the procedure as de- veloped by Langford et al. and Giannuzzi et al. [20-21] . Table 1 out- lines the parameters for sample preparation. Both EBID-Pt and ion beam-induced deposition (IBID)-Pt are deposited over an area of approximately 2 μm × 22 μm, using the standard Zeiss deposition mode setting, as shown in Fig. 3 (a) and (b). The electron and ion beam voltages and currents used are 5 kV 3 nA and 30 kV 20 pA respectively. A large area of deposited Pt is needed to fabricate an extra-long lamella, which provides a large cross section for the microgrippers to handle. Large trapezoid trenches are milled us- ing the mill for depth setting on each side of the lamella. These trenches have approximate dimensions of top length: 40 μm, bot- tom length: 50 μm, trench width: 15 μm and trench depth: 15 μm, Fig. 3 (c). The side trench (30 μm × 10 μm) is milled using the mill for depth setting with an approximate depth of 15 μm. All are per- formed at a tilt of 54 °. The undercut (1 μm × 24 μm) is performed at a tilt of 7 °. It is milled using the mill for time setting until the undercut is clearly visible, see Fig. 3 (d). All milling was performed at an ion beam voltage of 30 kV 4 nA with the exception of the undercut, which was performed at 30 kV 2 nA.

After the bulk of the lamella is prepared, the microgrippers are inserted to lift the lamella away from the substrate to perform fine polishing. The rotating microgrippers are inserted near the bulk lamella. Before reaching the lamella, the grippers are opened to allow for the lamella to easily fit between them.

By switching between both SEM and FIB imaging, the lamella is placed between the microgrippers. Once in the correct position, the grippers are carefully closed until they begin to slide along the lamella, indicating that the lamella is secure. The remaining side- wall connected to the bulk is removed using the mill for depth setting with dimensions of 2 μm × 2 μm at an ion beam voltage of 30 kV 2 nA, Fig. 4 (b).

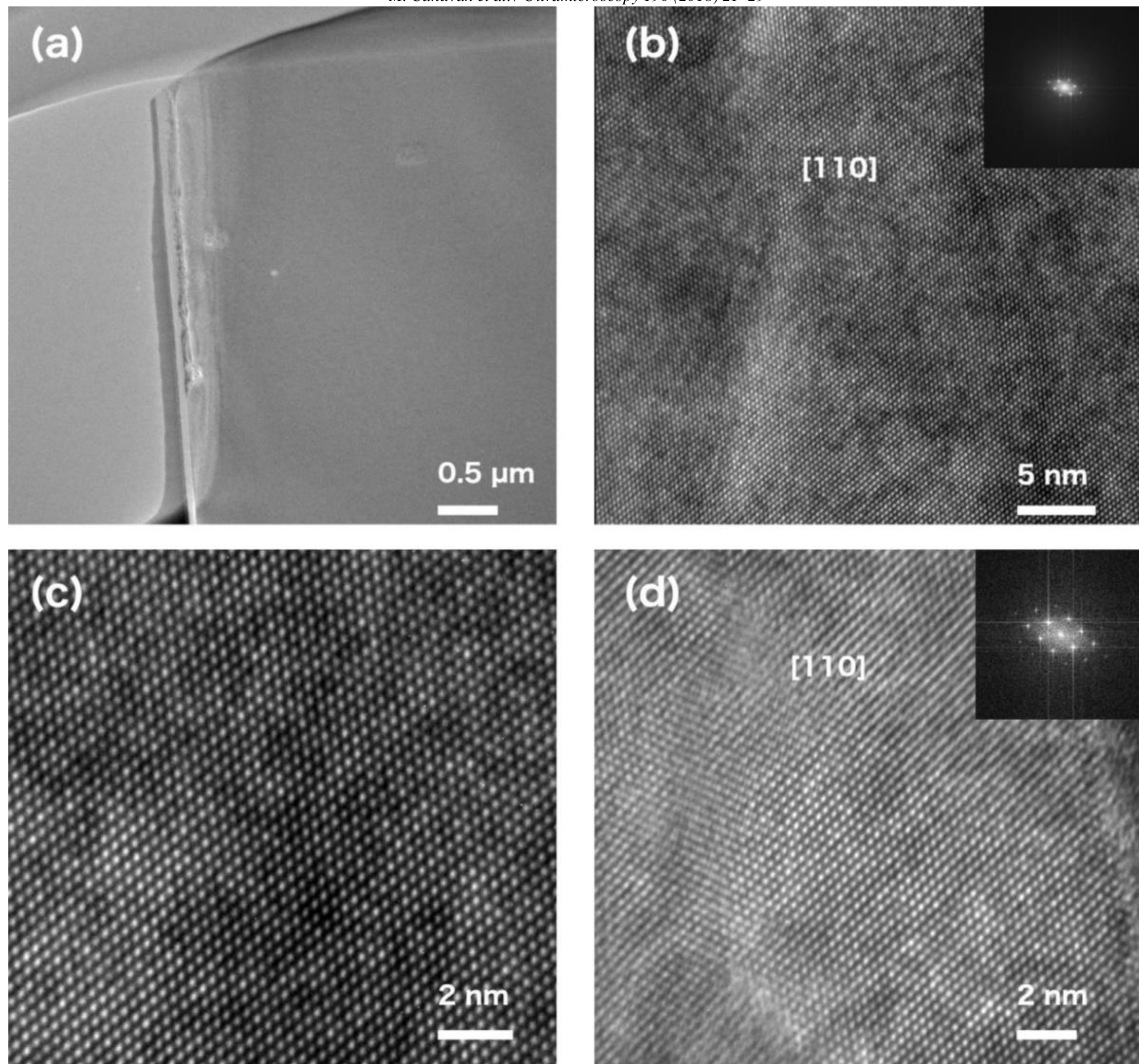

Fig. 7. (a) TEM image of lamella remains in desired position over through-hole window, (b) HRTEM of Si with FFT inset, (c) high magnification image of Si and (d) reference HRTEM image of Si substrate prepared using traditional in-situ lift-out technique with Pt weld with FFT inset.

Release of the lamella from the substrate is realised by a slight shift in the lamella position with respect to the bulk. The micro- grippers are tightened to ensure the lamella is securely gripped and slowly lifted out of the trench. When the lamella is lifted clear of the bulk, the substrate is moved away from the lamella/gripper by lowering the stage, Fig. 4 (d).

Fine thinning of the lamella is critical to enable high resolution imaging in the TEM. Using the rotating micrograppers, the lamella is tilted between 3 °–5 ° with respect to the FIB. The lamella is milled by adopting a wedge technique, as developed by Schaffer et al. This technique utilises a range of decreasing ion beam ener- gies, from 30 kV 240 pA–5 kV 20 pA, see Table 1 ., to ensure min- imal damage and amorphisation of the sample, and also to min- imise the loss of the Pt layer as the ion beam energies are reduced [22] . As can be seen from Fig. 5 (a), a staggered approach in relation to the top-down profile of the lamella

100 nm thickness. The accelerating voltage is reduced to 3 kV and the lamella is polished further until it is approximately 50–70 nm thick, Fig. 5 (d).

The use of the RoTip microgrippers provides many advantages over conventional methods [24] . The lamella can be milled and polished (front and back) without the obstruction of the MEMS de- vice itself and removes potential damage to the area surrounding the MEMS device window. The microgrippers also ensure there is no sputtering or re-sputtering of Pt due to welding, as no Pt weld is needed.

When the lamella is polished to a thickness of ~70 nm, the stage is tilted back to 0 ° and the MEMS device is brought to the SEM/FIB coincidence point. Having the stage at 0 ° tilt ensures the lamella will be in a more favourable position to lie flat over the window of the MEMS device, as the angle between the top of the lamella and the device surface is reduced below 90 °, see Fig. 6 (d).

is also employed. The stag- gered approach isolates parts of the lamella from the ion beam ex- posure during the thinning process, providing support to the thin regions. This also creates a ledge between the thinned area of in- terest of the lamella and the MEMS device. This approach elevates the area of interest while maintaining a parallel geometry between the MEMS device window and the lamella surface.

The thickness of the sample can be estimated by Secondary Electron (SE) imaging [23] . As the thickness of the specimen de- creases, the SE yield increases. The net result is a significant bright- ness increase in the SE signal as the specimen thickness is re- duced, highlighted region shown in Fig. 5 (d). While imaging with a 5 kV accelerating voltage, the area of interest is thinned to approx- imately 70–

To minimise charging between the sample, microgripper and MEMS device, the SEM accelerating voltage is kept at 3 kV, and the beam current reduced to ~10 pA. Furthermore, this prevents the SEMGlu from curing/hardening before the lamella is placed over the window.

The lamella is positioned above a window in the centre of the MEMS device and slowly lowered until the base of the lamella is in contact with the SiN_x surface. It is critical that the lamella is placed in the centre of the device where the temperature measure- ment is most accurate (the variation from the centre to the edge is ~15%) [25] . The thick part of the lamella gripped by the micro- grippers is placed directly over the SEMGlu, with the thinned area of interest extending over the adjacent through-hole window. To release the lamella, the microgrippers are

slowly opened while si- multaneously moving them in the x and y direction. In the closed position the microgrippers can be used to make minor adjustments to positioning of the lamella, which lies flat over the window. A short video clip demonstrating the complete lift-out and polishing procedure is available in the Supplementary Information.

To secure the lamella in the desired position, the microgrippers are pressed against the thick side of the lamella away from the window. The SEMGlu beneath the thick section is cured by increas- ing the acceleration voltage to 30 kV with an electron beam current of ~6 nA with a field of view of approximately 100 μm^2 and ex- posing the area for 30 minutes. This process results in a securely bound lamella to the MEMS device, providing a robust platform for *in-situ* TEM analysis.

Fig. 7 shows TEM images of the thinned region extending over the electron transparent window, after sample transfer to the *in- situ* holder and TEM. From a comparison between the SEM image in Fig. 6 (b) and the TEM image in Fig. 7 (a), the lamella remains in the desired position with no movement evident. This demonstrates the mechanical robustness of the SEMGlu as well as the vacuum-compatibility within the TEM.

Fig. 7 (b) shows the high resolution TEM image of the Si (110) substrate recorded from the thin region of the lamella. From the TEM image and Fast Fourier Transform (FFT) it is clear that the sample remains crystalline with no apparent damage after ion- beam polishing. These results are what we expect from lamellae prepared by traditional *in-situ* lift-out techniques, Fig. 7 (d). It is evident that lamellae prepared using this novel technique main- tain the same quality while removing the risk of Pt re-deposition as well as the risk of damaging the MEMS device through milling.

4. Summary and conclusions

An alternative *in-situ* lift-out procedure using focused ion beam milling was developed and optimised for the preparation of lamel- lae for *in-situ* annealing in the transmission electron microscope and beyond.

This technique combines for the first time the use of rotating microgrippers for lift-out and thinning, and a unique adhesive sub- stance, SEMGlu, during the lift-out procedure, instead of the tradi- tional micromanipulator needle and Pt weld. Lamellae were suc- cessfully mounted onto a MEMS device for *in-situ* TEM annealing experiments without damage to the MEMS.

It has been shown that this novel method ensures the ability to employ the wedge technique during the thinning procedure due to the rotation of the microgrippers. The use of the microgrippers also ensured no Pt deposition onto the sample and reduced the risk of damaging the MEMS device during thinning.

HRTEM imaging of the polished lamella verifies that this method can produce high quality lamellae comparable with reg- ular *in-situ* lift-out procedures.

Not only is the method successful for *in-situ* annealing, it can also be used and adapted for a number of *in-situ* applications, such as fluid and gas analysis as well as *in-situ* electrical experimenta- tion and also traditional lamella preparation.

Author contribution

MC, DD, CMcA and VN conceived the project. MC developed the technique along with DD, AR and CMcA. MC and EMcC performed in-situ annealing TEM experiments. MC wrote the paper with con- tributions from all authors in the discussion and preparation of the manuscript.

Acknowledgements

MC wishes to acknowledge the Advanced Microscopy Labora- tory (AML), CRANN, Trinity College Dublin. All imaging and anal- ysis pertaining to the main text was carried out at the AML at the AMBER centre, CRANN Institute, Trinity College Dublin, Ireland. AML is an SFI supported imaging and analysis centre. MC wishes to thank Dr. Edmund Long for his contribution to the prepara- tion of this manuscript. MC wishes to thank the Irish Research Council for their support. VN wishes to acknowledge the support of the European Research Council (2DNanoCaps, 3D2DPrint, TC2D), Science Foundation Ireland (PIYRA Award, AMBER and I-Form Cen- tres) and H2020 (MoWSeS and CoPilot).

Conflict of Interest None.

References

[1] P.J. Ferreira , K. Mitsuishi , E.A. Stach , In Situ transmission electron microscopy, MRS Bull. 33 (February (2)) (2008) 1–8 .

[2] R. Dannenberg , E. Stach , J.R. Groza , B.J. Dresser , TEM annealing study of normal grain growth in silver thin films, Thin Solid Films (December (379)) (20 0 0) 133–138 .

[3] R.J. Kamaladasa , A .A . Sharma , Y.-T. Lai , W. Chen , P.A . Salvador , J.A . Bain , M. Skowronski , Y.N. Picard , In situ TEM imaging of defect dynamics under electrical bias in resistive switching rutile-TiO_2 , Microsc. Microanal. (February) (2015) 1–14 .

[4] K. Tai , Y. Liu , S.J. Dillon , In situ cryogenic transmission electron microscopy for characterizing the evolution of solidifying water ice in colloidal systems, Microsc. Microanal. 20 (February (2)) (2014) 330–337 .

[5] H. Zheng , S.A. Claridge , A .M. Minor , A .P. Alivisatos , U. Dahmen , Nanocrystal diffusion in a liquid thin film observed by in situ transmission electron mi- croscopy, Nano Lett. 9 (June (6)) (2009) 2460–2465 .

[6] M.J. Williamson , R.M. Tromp , P.M. Vereecken , R. Hull , F.M. Ross , Dynamic mi- croscopy of nanoscale cluster growth at the solid–liquid interface, Nat. Mater. 2 (July (8)) (2003) 532–536 .

[7] J.F. Creemer , S. Helveg , G.H. Hoveling , S. Ullmann , A.M. Molenbroek , P.M. Sarro , H.W. Zandbergen , Atomic-scale electron microscopy at ambient pressure, Ul- tramicroscopy 108 (August (9)) (2008) 993–998 .

[8] M. Legros , D.S. Gianola , K.J. Hemker , In situ TEM observations of fast grain-boundary motion in stressed nanocrystalline aluminum films, Acta Ma- terialia 56 (August (14)) (2008) 3380–3393 .

[9] N. Li , H. Wang , A. Misra , J. Wang , In situ nanoindentation study of plas- tic co-deformation in Al-TiN nanocomposites, Sci. Rep. 4 (October (1)) (2014) 6537–6538 .

[10] J.Y. Huang , H. Choi , D. Takahashi , K. Kono , E. Kim , In situ observation of the electrochemical lithiation of a single SnO_2 nanowire electrode, Science 330 (December (6010)) (2010) 1512–1515 .

[11] H. Saka , T. Kamino , S. Arai , K. Sasaki , In situ heating transmission electron mi- croscopy, MRS Bull 33 (February (2)) (2008) 1–8 .

[12] M. Miyasaka , K. Makihira , T. Asano , E. Polychroniadis , J. Stoemenos , In situ ob- servation of nickel metal-induced lateral crystallization of amorphous silicon thin films, Appl. Phys. Lett. 80 (6) (2002) 944 .

[13] A. Rath , R.R. Juluri , P.V. Satyam , Real time nanoscale structural evaluation of gold structures on Si (100) surface using in-situ transmission electron mi- croscopy, J. Appl. Phys. 115 (May (18)) (2014) 184303–184307 .

[14] R. Dannenberg , E.A. Stach , J.R. Groza , B.J. Dresser , In-situ TEM observations of abnormal grain growth, coarsening, and substrate de-wetting in nanocrys- talline Ag thin films, Thin Solid Films 370 (July (1)) (20 0 0) 54–62 .

[15] L.F. Allard , W.C. Bigelow , M. Jose-Yacaman , D.P. Nackashi , J. Damiano , S.E. Mick , A new MEMS-based system for ultra-high-resolution imaging at elevated tem- peratures, Microsc. Res. Tech. 72 (March (3)) (2009) 208–215 .

[16] N.P. Young , M.A. van Huis , H.W. Zandbergen , H. Xu , A.I. Kirkland , Transfor- mations of gold nanoparticles investigated using variable temperature high- -resolution transmission electron microscopy, Ultramicroscopy 110 (March (5)) (2010) 506–516 .

[17] M.A. van Huis , N.P. Young , G. Pandraud , J.F. Creemer , D. Vanmaekelbergh , A.I. Kirkland , H.W. Zandbergen , Atomic imaging of phase transitions and mor- phology transformations in nanocrystals, Adv. Mater. 21 (October (48)) (2009) 4 992–4 995 .

[18] R.M. Langford , M. Rogers , In situ lift-out: steps to improve yield and a compar- ison with other FIB TEM sample preparation techniques, Micron 39 (December (8)) (2008) 1325–1330 .

[19] D. Tomus , H.P. Ng , In situ lift-out dedicated techniques using FIB–SEM system for TEM specimen preparation, Micron 44 (January) (2013) 115–119 .

[20] R.M. Langford , A.K. Petford-Long , Preparation of transmission electron mi- croscopy cross-section specimens using focused ion beam milling, J. Vac. Sci. Technol. A 19 (5) (2001) 2186 .

[21] L.A. Giannuzzi , J.L. Drown , S.R. Brown , R.B. Irwin , F.A. Stevie , Focused ion beam milling and micromanipulation lift-out for site specific cross-section tem spec- imen preparation, MRS Proc. 480 (January) (1997) 19–27 .

[22] M. Schaffer , B. Schaffer , Q. Ramasse , Sample preparation for atomic-resolution STEM at low voltages by FIB, Ultramicroscopy 114 (March) (2012) 62–71 .

[23] R.M. Langford , C. Clinton , In situ lift-out using a FIB-SEM system, Micron 35 (October (7)) (2004) 607–611 .

[24] M. Duchamp , Q. Xu , R.E. Dunin-Borkowski , Convenient preparation of high- -quality specimens for annealing experiments in the transmission electron mi- croscope, Microsc. Microanal. 20 (November(6)) (2014) 1638–1645 .

[25] L. Mele , F. Santagata , E. Iervolino , M. Mihailovic , T. Rossi , A.T. Tran , H. Schelle- vis , J.F. Creemer , P.M. Sarro , A molybdenum MEMS microhotplate for high-tem- perature operation, Sens. Actuat. 188 (Decemeber) (2012) 173–180 .

[26] A. Rummel , G. Frayne , A.J. Smith , S. Kleindiek , Achieving fast and reliable TEM-sample lift-out and transfer using novel materials and novel in-situ tools, Prakt. Metallogr. (May) (2009) 1–5 .